Adsorption of volatile organic and iodine compounds over silver-exchanged mordenites A comparative periodic DFT study for several silver loadings

H. Jabraoui, E.P. Hessou, S. Chibani, L. Cantrel, S. Lebègue, M. Badawi

Version of Record: https://www.sciencedirect.com/science/article/pii/S0169433219309134
Manuscript_10be517f10319f2357d3fa0746c4c895

Adsorption of Volatile Organic and Iodine Compounds Over Silver-Exchanged Mordenites: A Comparative Periodic DFT Study for Several Silver Loadings

H. Jabraoui[a], E. P. Hessou[a], S. Chibani[b], L.Cantrel[c], S. Lebègue[a], M. Badawi[a,*]

[a] Laboratoire Physique et Chimie Théoriques, UMR 7019, CNRS - Université de Lorraine, F-54000 Nancy, France.

[b] Unité de Catalyse et de Chimie du Solide, UMR 8181, Univ. Lille, CNRS, ENSCL, Centrale Lille, Univ. Artois, F-59000 Lille, France.

[c] Institut de Radioprotection et de Sûreté Nucléaire, PSN-RES, CEA Cadarache, F-13115 Saint Paul lez Durance, France

* Corresponding author: michael.badawi@univ-lorraine.fr

ABSTRACT

The ability of Ag-exchanged mordenite (Ag-MOR) to capture iodine species such as I_2 and CH_3I as released for instance during a nuclear accident can be severely limited by the presence of volatile organic compounds (VOCs) that can disrupt their adsorption in the zeolite. Here, using density functional theory (DFT), we investigate in detail the adsorption process of several hydrocarbons (methane, cyclohexane, benzene, and 1,3-dimethylbenzene) and oxygenated compounds (methanol, ethanol, propan-2-ol and propanone) and compare it with the adsorption of I_2 and CH_3I for different values of the Si/Al ratio of the Ag-exchanged mordenite. It is found that the adsorption process of the iodine species becomes favorable as the Si/Al ratio is decreased. Indeed at high Si/Al ratio, some VOCs such as benzene, 1, 3-dimethylbenzene and propan-2-ol exhibit strong inhibiting effects, while at low Si/Al ratio, only the adsorption of CH_3I is limited by the presence of aromatic hydrocarbons. Also, in addition to the elongation of the I-I bond upon the adsorption of the iodine molecule in Ag-MOR with a high silver content, we found that there is a significant electron transfer between the Ag and I atoms. Thus, our results indicate that the I-I bond becomes weaker during the adsorption and therefore the formation of AgI precipitates is favored.

1. Introduction

During a core meltdown accident in a nuclear power plant, the iodine species CH_3I and I_2 may be released to the atmosphere, resulting in negative health effects directly related to radiation[1] due to their relatively easy assimilation by thyroid. Many efforts have been made to confine these species and limit their spread in the environment. In other words, the effective capture of iodine compounds is of great importance in terms of public safety. Nowadays, a common strategy to trap gaseous iodine-containing compounds involves the iodine precipitation by using porous solids [2,3] such as polymers [4], nanocomposites [5], metal-containing systems [6], and zeolites [7-11]. The latter exhibit appealing features such as a high removal efficiency, simple equipment design, and a low maintenance cost.

Among the most efficient porous sorbent materials, silver-exchanged zeolites present the unique ability to strongly capture iodine species by the formation of AgI precipitates [12,13]. Indeed, Chapman and coworkers [14] employed a differential approach for the analysis of the pair distribution function (PDF) of an I_2-treated Ag-MOR, and they reported the structure and distribution of AgI correlated to the iodine trapping. To explore deep this phenomenon, Azambre and Chebbi [15] studied different silver exchange zeolites (Faujasite X and Y, Mordenite, *BEA, MFI, FER) to probe the relationships between chemical, structural and textural parameters, as well as their iodine trapping efficiencies (CH_3I). They observed the formation of AgI for all silver zeolites as well as the fact that the amount of AgI precipitates is directly related to the silver content. Moreover, Chapman et al [14] reported that Ag-MORs represent an important safe pathway for radioactive iodine capture since they present the ability of using pore-blockage to further trap the iodine for long-term storage. All these characteristics make Ag-MORs used for iodine trapping under mild operating conditions in nuclear fuel reprocessing facilities [14, 16, 17]. However, their disadvantages are the high cost of silver and the possible inhibiting effect of gaseous species on the adsorption of the iodine species [9,18-20].

Among the potential inhibiting species formed during nuclear severe accidents [21,22], we can find some VOCs such as aromatics (benzene, 1.3-dimethylbenzene), ketone (2-propanone), alcohols (ethanol, methanol, 2-propanol), and alkane (methane, cyclohexane) as suggested by Jolley et al [9]

The possible source of organic molecules are numerous in nuclear power plants such as paints containing solvents [23], polymers (electric cables) and oils.

However to our knowledge, there is no experimental data concerning the possible inhibiting effect of these molecules on the trapping of iodine on silver zeolites. Indeed, some theoretical works have been recently published [18-20], confirming that other contaminants such as CO or H_2O can inhibit the adsorption of the iodine species. In this context, Chebbi and coworkers [20] reported the inhibiting effect of CO on the I_2 adsorption on Ag-exchanged faujasite (Ag-FAU), while Chibani evidenced the inhibiting effects of CO and H_2O on I_2 and CH_3I trapping by Ag-MOR [18]. Remarkably, the inhibiting effect of the former contaminants could be considerably limited when the Si/Al ratio decreases [19].

The objective of this work is to study if some organic contaminants that exist in nuclear installations are capable to inhibit the capture of iodine species. To this aim, we have used DFT to assess the inhibiting effects of the following VOCs: methane (CH_4), cyclohexane (C_6H_{12}), benzene (C_6H_6), 1,3-dimethylbenzene (C_8H_{10}), methanol (CH_3OH), ethanol (C_2H_5OH), propan-2-ol (C_3H_7OH), and propanone (C_3H_6O), on the iodine trapping into Ag-MOR. Three Si/Al ratios for the Ag-MOR have been considered on the basis of experimental data: Si/Al = 5, 11, and 47 [21].

The paper is organized as follows: first, we detail our computational procedure, then, the obtained results with Ag-MOR for several Si/Al ratios are presented and discussed with a focus on the potential inhibiting effect of the VOCs on the trapping of iodine species, and finally we outline the main conclusions of our study.

2. Computational details

2.1. Structural models

The considered mordenite framework displays three different types of cavities: the main channel (MC), the side channel (SC), and the side pocket (SP). The MC is obtained from 12-membered rings stacked in a parallel array along the c-axis. The SP is accessible from the MC through 8-membered

rings (more details are available in Ref 19). The MC has a large aperture to accommodate molecules of aromatic sizes [24,31] as well as the adsorption of iodine molecules is favored in this channel compared to the SC and SP [18,25].

To obtain Ag-MORs, some silicon atoms are substituted by aluminum atoms to create a negative charge, allowing to add the silver cation. In the literature, the pure siliceous mordenite conventional cell contains 144 atoms (48 Si and 96 O) [26], exhibiting an orthorhombic structure (space group: Cmcm) with lattice parameters: a = 18.094 Å, b = 20.516 Å and c = 7.524 Å. Here our Ag-MORs structure are based on the structure optimized by Bucko et al [27] with the primitive monoclinic cell doubled in the c-direction, its lattice parameters are estimated at a=b=13.805 Å, c = 15.212 Å and $\beta = 82.81°$. Based on previous works [18, 19] which systematically analyzed the distribution of Al and Ag atoms inside Ag-MOR, we have selected the most energetically stable site of the MC, namely T1- E according to the Mortier's [28] classification. This location is the most frequently occupied by cations [28], and has been also chosen in other theoretical investigations [29, 30, 31].

2.2. Periodic density functional theory calculations

The adsorption of iodine and organic compounds onto Ag-zeolites is investigated using the Vienna Ab-initio Simulation Package (VASP) [32]. These calculations employed the PBE functional [33] and the PAW method developed by Blöchl [34] and later adapted by Kresse and Joubert [35]. The plane wave cutoff energy has been set to 450 eV and a Gaussian smearing σ = 0.1 eV is used to help the convergence. Atomic positions are fully optimized up to all forces are less than 0.02 eV / Å per atom. The Kohn–Sham equations were solved self-consistently until the energy difference between cycles take a value smaller than 10^{-6} eV. The Brillouin-zone sampling was restricted to the Γ-point. The considered dispersion correction scheme in our calculations is the Tkatchenko–Scheffler scheme with iterative Hirshfeld partitioning [36,37] as implemented in VASP by Bucko et al [37,38] So far, this method shows promising results to describe adsorption phenomena onto zeolites [18,19,37,38].

The adsorption phenomena can be evaluated using the interaction energy of zeolite-adsorbate, which can be expressed using the combination of the following three terms:

$$\Delta E_{int} = E_{zeolite-X} - E_{zeolite} - E_X \quad (1)$$

Where:

- $E_{zeolite}$: the energy of the clean MOR;
- E_X: the energy of the isolated molecule in gaseous phase;
- $E_{zeolite\text{-}X}$: the energy of MOR with adsorbed molecules;

Also, the dispersion energy contribution ΔE_{disp} to the interaction energy is obtained as:

$$\Delta E_{disp} = E_{disp\ zeolite-X} - E_{disp\ zeolite} - E_{disp\ X} \quad (2)$$

To further improve our understanding of the nature of the bonding interactions, we have determined the difference in electronic density ($\Delta\rho$) and the difference in Bader charge (ΔQ). To visualize the charge density difference ($\Delta\rho$) (using VESTA [39]) upon adsorption of molecules into MOR, we have calculated the charge densities of the clean MOR ($\rho_{zeolite}$), of the isolated molecule in the gaseous phase (ρ_x), and of the MOR with adsorbed molecules ($\rho_{zeolite\text{-}X.}$). Then to get ($\Delta\rho$), we have used the following expression:

$$\Delta\rho = \rho_{zeolite\text{-}X} - \rho_{zeolite} - \rho_X \quad (3)$$

The Bader approach consists in partionning the electronic density of a system in different volumes which when integrated over space, can provide the charge of an atom [40-43]. To get the difference in electronic charge ΔQ, we have computed the Bader charge for each atom (Z) in the zeolite-X, in the clean zeolite and in the isolated molecules.

$$\Delta Q = Q_{\text{Atom Z in zeolite-X}} - Q_{\text{Atom Z in zeolite or X}} \quad (4)$$

Where:

$Q_{\text{Atom Z in zeolite-X}}$: the Bader charge for all the atoms in the MOR with adsorbed molecules.

$Q_{\text{Atom Z in zeolite or X}}$: the Bader charge for all the atoms in the clean zeolite or in the isolated molecule in gaseous phase.

3. Results and discussions

Herein, we report the potential impact of certain species of VOCs on the removal of iodine released in nuclear waste. We have classified the investigated VOCs into two categories as follows:

- Hydrocarbons: benzene (C_6H_6), 1,3-dimethylbenzene (C_8H_{10}), cyclohexane (C_6H_{12}), and methane (CH_4).
- Oxygenated hydrocarbons: methanol (CH_3OH), ethanol (C_2H_5OH), propan-2-ol (C_3H_7OH), and propanone (C_3H_6O).

Our computed interaction energies of the iodine molecules and VOCs with Ag-MORs (Si/Al = 5, 11, and 47) are presented in Table 1. We also verified the dissociative adsorption and then confirmed that there was no dissociation observed in the studied molecules (see supporting information, the case of alcohol molecules).

3.1 Iodine species

Regarding the interactions between iodine species and Ag-MOR as a function of Si/Al ratio, we found that they increase as the Si/Al ratio decreases, especially in the case of I_2. Indeed, as indicated in Table 1, the total interaction energies of I_2/CH_3I are -132.6/-152.1 kJ/mol for Si/Al = 47, -183.8/-151.8 kJ/mol for Si/Al = 11, and -297.6/-188.5 kJ/mol for Si/Al = 5, in line with an increase of the I-I bond length. Concerning Ag-MOR with Si/Al = 47, each iodine atom of I_2 or of CH_3I interacts with an Ag atom. Here CH_3I is more adsorbed than I_2 by around 30 kJ/mol. However, for Si/Al = 11 and 5, the molecule of I_2 is more adsorbed than CH_3I by an amount of about 30 kJ/mol and 109 kJ/mol, respectively. Let us now explain these trends: for the adsorption CH_3I, the atom of I interacts with 2 atoms of Ag located on the same side in the main channel for Si/Al = 11 and 5 (see Fig.1), which leads to similar interaction energy for both Si/Al ratio. The I-CH_3 distance does not evolve upon the adsorption of CH_3I whatever the Si/Al ratio, suggesting that the dissociation of iodomethane would be

more difficult than the one of molecular iodine under these conditions. Indeed, in the case of I_2, we can find that its atoms can interact with more silver atoms (4 Ag atoms for Si/Al = 11 and at least 6 Ag atoms for Si/Al = 5 see Fig. 1), which leads to a significant increase in its total interaction energy (50 kJ/mol for Si/Al =11 and 120 kJ/mol for Si/Al =5) compared to its adsorption into Ag-MOR for Si/Al = 47. Besides, the long-range dispersion contributions of both I_2 and CH_3I in to their total interaction energies present almost the same values. So, the difference can come from the DFT contributions to the overall interaction energies: the corresponding values for I_2 are always higher than those of CH_3I irrespective of the Si/Al ratio.

The increase of the total interaction energy with the decrease of the Si/Al ratio can be understood by studying the electron density ($\Delta\rho$) and Bader charge (ΔQ) differences induced by the adsorption. In this vein, we found that the interactions between I and Ag atoms present a significant electron transfer, where a high Ag content (Si/Al = 5) results in a large charge transfer between the Ag atoms and the iodine atoms of I_2 (See Fig.1). For the ratio 5, our calculated Bader charges (see, Table SI-2), show that the iodine atoms bear the largest positive charge (+0.15e) and the Ag atoms bonded directly to the iodine bear a negative charge. In other word, iodine atoms pick up electrons during the adsorption process. For all the rest of the atoms, the Bader charge are almost unaffected by the adsorption of I_2. However, upon adsorption of CH_3I, the iodine atoms always carry a negative charge of -0.24e (see, Table SI-2) and -2.21e for Ag-MOR (Si/Al=5) and Ag-MOR (Si/Al=47), respectively. Overall, these findings indicate that the I-I bond in I_2 becomes weak upon adsorption, which could promote the formation of AgI precipitates as explained by Bucko et al [44].

3.2. Hydrocarbons

3.2.1. Aromatic molecules

We found that the interaction energies of aromatic compounds increase when the Si/Al ratio decreases. Indeed, the total interaction energies of benzene/1,3-dimethylbenzene are -155.8/-183.3 kJ/mol in the case of Si/Al = 47, -185.1/-219.9 kJ/mol for Si/Al = 11 and -219.4/-254.3 kJ/mol for Si/Al = 5 (See Figure 2 and Table 1). The long-range dispersion contributions of benzene/1,3-dimethylbenzene are

41/51% for Si/Al = 5, 42/51% for Si/Al = 11, and 47/50% for Si/Al = 47. We note that these molecules have almost the same contribution regardless of the Si/Al ratio (about 50%). These results show that about half of the interaction between benzene or 1,3-dimethylbenzene and Ag-MORs is due to dispersion forces. This contribution can be correlated with π-cation interactions, which are ubiquitous in systems involving aromatic compounds and metallic ions as has been confirmed by different theoretical [45,46,47] and experimental [48,49] investigations. Generally, aromatic molecule adsorptions on cations are particularly interesting in view of the participation of π-electrons in the total interaction. Benzene and its derivatives can form a variety of charge-transfer complexes depending on their ability to donate electrons or to accept electrons[50].

In this regard, Kozyra et al [51] have studied the π-cation interactions between benzene and Ag sites in ZSM-5, where a large charge transfer from benzene to Ag occurs. This is in line with our own results as a significant electron transfer between benzene or 1,3-dimethylbenzene and Ag-MOR is observed for all the tested Si/Al ratios and especially with the ratio 5, see Fig. 3. For the latter ratio, benzene and 1,3-dimethylbenzene exhibit for most composed atoms positive Delta Q (Table SI-2), highlighting their important interaction with the MOR structure.

To discuss the adsorption of both aromatic molecules into Ag-MORs in term of geometric parameters and with π-cation interactions [52-54], we have reported in Table 2 the distances between the silver atoms and the center of the aromatic rings. For Si/Al = 47, a single Ag atom interacts with the aromatics rings of benzene and 1,3-dimethylbenzene at a distance of 2.66 Å and 2.74 Å, respectively. Here, the 1,3-dimethylbenzene molecule is more adsorbed than benzene by around 27 kJ/mol. For Si/Al = 11, the adsorption of 1,3-dimethylbenzene into Ag-MOR is achieved through the interaction between its aromatic ring and one Ag atom at a distance of 2.68 Å. In contrast, for the benzene adsorption into Ag-MOR for Si/Al = 11, there are 2 Ag atoms bonded to the aromatic ring at distances of 2.89Å and 3.17Å, which show that the adsorption of 1,3-dimethylbenzene is stronger than with benzene by around 34 kJ/mol.

In the case of Ag-MOR for Si/Al=5, 1,3-dimethylbenzene and benzene interact with two and three silver atoms, respectively. The reported distances are 2.73 Å and 2.79 Å for 1,3-dimethylbenzene and 3.09 Å, 3.13 Å and 3.27 Å for benzene (see Table 2) . In this case, the 1,3-dimethylbenzene is more

adsorbed than the benzene molecule by around 43 kJ/mol. Fig. 3 is showing the electron transfers occurring upon adsorption of benzene and 1,3-dimethylbenzene in Ag-MORs (see Fig.3).

3.2.2. Cyclohexane

Regarding the influence of the Si/Al ratio on cyclohexane-Ag interactions, the total interaction energy of cyclohexane is equal to -173.2 kJ/mol for Si/Al = 5 while it is -153.9 kJ/mol for Si/Al = 11, and -120.3 kJ/mol for Si/Al = 47. Here, we found that cyclohexane having no π-electrons is mainly adsorbed by dispersion forces whatever the Si/Al ratio. This result is in a good agreement with reported by Suda et al [55], who have experimentally investigated the adsorption of benzene, cyclohexene, and cyclohexane on the surface of titanium dioxide.

As reported by Barthomeuf et al [56], cyclohexane and benzene have the same number of carbon atoms and similar polarizabilities, but differ in that benzene can give rise to specific interactions between its aromatic ring and cations in zeolites. In our work, we found that benzene is more adsorbed than cyclohexane (which have no π-electrons) by around 46 kJ/mol in Ag-MOR (Si/Al=5), 31 kJ/mol in Ag-MOR (Si/Al=11), and 36 kJ/mol in Ag-MOR (Si/Al=47). So, the benzene π-electrons contribute to the increase of total interaction energy. While zeolites have localized charges that render their surface heterogeneous [57], it can be assumed that the cyclohexane-silver interactions are weak enough to permit the adsorption of cyclohexane on an apparently homogeneous surface.

3.2.3. Methane

The total interaction energy of methane is -46.6 kJ/mol for Ag-MOR (Si/Al = 5), -40.5 kJ/mol for Ag-MOR (Si/Al = 11), and -45.5 kJ/mol for Ag-MOR (Si/Al = 47). We can remark that the total interaction energy has almost the same values for all used Si/Al ratios in Ag-MOR. Also, the dispersion energy increases to -25.1 kJ/mol for Si/Al = 5 against -21.8 kJ / mol for Si/Al = 11, and -17.0 kJ/mol for Si/Al = 47. Therefore at low Ag content in Ag-MOR, the adsorption of methane is mainly directed by short range interactions (more than 62% of the total interaction energy). In contrast,

the methane adsorption is mainly achieved through dispersion energy (long-range interaction) when the silver content of the zeolite is high (54%).

3.3. Oxygenated hydrocarbons

The effect of the Ag content in Ag-MOR on the oxygenated molecules adsorption is also studied. We choose as case studies the alcohols: methanol, ethanol, propan-2-ol, and propanone. The interaction energies of methanol/ethanol/propan-2-ol goes from -117.6/-146.4/-164.0 kJ/mol (for Si/Al = 5 to -106.5/-125.3/-147.7 kJ/mol for Si/Al = 47, and it increases with the carbon atoms number (See Fig.5), suggesting that there exists a linear function relating the interaction energy variation with respect to the carbon atoms number (nC) of the studied alcohols, which can be expressed as follows:

$$\Delta E_{int}(nC) = a(nC) + b \quad (3)$$

Where "a" and "b" represents the contribution of dispersion and DFT energies to the total interaction energy, respectively. To combine the different contribution reported in Table 1 and in Eq.3, we can identify the different energetic terms contributing to the adsorption of each alcohol. Table 3 shows the dispersion and DFT contributions of the carbon and oxygen atoms to the adsorption of the investigated alcohols. Thus, these findings indicate that the high adsorption of alcohols is directly related to the carbon chain. Indeed, going from one alcohol to another by adding a carbon, one can estimate an increase of the interaction energy to be ~20 kJ/mol.

The comparison of the C-O distance of alcohols before and after their adsorption enable us to evaluate the occurrence of C-O bond breaking upon adsorption and therefore the possibility of formation of undesirable byproducts that can affect the adsorption of iodine species. We found that this distance in methanol/ethanol/propan-2-ol varies from to 1.44 Å (gaseous phase, for all alcohol molecules) to about1.45 Å/1.45 Å/1.48Å (adsorbed state) for every Si/Al ratio (See Table 3 and Fig. SI-2). Therefore the propanol is expected to react upon adsorption much more than methanol or ethanol.

The adsorption of propanone in Ag-MOR prefers to be via its oxygen atoms. So, as Si/Al ratio decreases in Ag-MOR, the total interaction energy raises to -158.4 kJ/mol (for Si/Al = 5) compared to

-142.7 kJ/mol (for Si/Al = 11) and -146.9 kJ/mol (for Si/Al = 47). On the other hand, we found that propan-2-ol is slightly more adsorbed than propanone by around 6.1 kJ/mol for Si/Al = 5, 16.8 kJ/mol for Si/Al = 11, and 0.8 kJ/mol for Si/Al = 47.

3.4. Effect of the Si/Al on the selective trapping of iodine species towards VOCs

For Ag-MOR with different Si/Al ratios, we have compared the adsorptions of the iodine species and the investigated VOCs as reported in Figure 2 and Figure 4. For each ratio, we show the most adsorbed VOCs and the less adsorbed iodine compound (I_2 for Si/Al = 47, CH_3I for Si/Al = 5 and 11) as follows:

- For Si/Al = 47, the most absorbed VOCs are 1,3-dimethylbenzene/benzene/propan-2-ol/propane and they present higher total interaction energies than I_2 by around ~ 50/23/15/14 kJ/mol, respectively.
- For Si/Al=11, 1,3-dimethylbenzene/benzene/cyclohexane/propan-2-ol are more adsorbed than CH_3I by around ~ 68/33/2/7 kJ/mol, respectively.
- For Si/Al = 5, the most strongly adsorbed VOCs are 1,3-dimethylbenzene/benzene, showing a total interaction energy higher than that of CH_3I by around ~ 37/30 kJ/mol.

In general, aromatic molecules potentially present the strongest inhibiting effects on the iodine removal compared to other VOCs. More precisely, benzene, 1,3-dimethylbenzene and propan-2-ol are expected to inhibit the adsorption of I_2 and CH_3I.

Moreover, we conclude that in Ag-MOR with a low Si/Al ratio, larger molecules such as I_2, benzene, 1,3-dimethylbenzene and propan-2-ol have total interaction energies that are 5-35% higher than in Ag-MOR with a high Si/Al ratio. This increase can be correlated with the increase in the number of cations interacting with those molecules. This behavior is clearly confirmed by the electronic density map (see Figs 1 and 3). In the opposite case, small molecules such as methane and CH_3I interact with almost the same number of cations, even though the Si/Al ratio decreases, resulting in the neglected effects of increasing cations on total interaction energies of these molecules.

However, decreasing the Si/Al ratio drastically limits the potential inhibiting effect of propan-2-ol on the adsorption of I_2 and CH_3I. Finally, the inhibiting effects of 1,3-dimethylbenzene and benzene on I_2 trapping are also limited for a low Si/Al ratio, but these effects are still present in the trapping of CH_3I.

4. Conclusion

Using periodic DFT calculations, we have investigated the interaction between Ag-MORs and different type of gaseous molecules which can be present in the atmosphere of a containment environment generated from a severe nuclear accident, with the aim to determine the influence of the Si/Al ratio on the adsorption selectivity of iodine compounds towards VOCs.

We have found that the adsorption of iodine species is strongly influenced by the Si/Al ratio variation in Ag-MOR. Indeed, the interaction energies of I_2 and CH_3I with Ag-MORs strongly increase when the silver content increases, i.e. the Si/Al ratio decreases. So, both CH_3I and I_2 prefer to be absorbed by Ag by their iodine I atom with at a distance I-Ag of 2.6 Å, which is accompanied by a large electron transfer between Ag atoms and I atoms. On the other hand, when the iodine molecule is absorbed in Ag-MOR for Si/Al = 5 and 11, the I-I bond is elongated. Thus, these results indicate that the I-I bond becomes weak upon adsorption and the formation of AgI precipitates could be favored.

Regarding the VOCs, the cyclohexane, benzene, 1,3-dimethylbenzene and propan-2-ol are more adsorbed than iodine species in Ag-MOR for Si/Al=47, and 11, which can play an inhibiting effect on the iodine trapping. For the considered aromatic molecules, benzene and 1,3-dimethylbenzene prefer to be absorbed on Ag^+ through π-electrons at a distance of Ag-aromatic center ranging from 2.65 Å to 3.16 Å. In the case of the alcohols, the investigated molecules are adsorbed via their oxygen atom at a distance of 2.2Å. This issue can be overcome by decreasing of the Si/Al ratio. However, even for a low Si/Al content in Ag-MOR, the problem of the inhibiting effects of benzene and 1,3-dimethylbenzene on the trapping of CH_3I is still present. Besides, methane exhibits a weaker

interaction with Ag-MORs than the other studied molecules, which means that methane shows no inhibiting effect on iodine trapping.

Our findings show that benzene, 1,3-dimethylbenzene and propan-2-ol (in a lesser extent) are the VOCs present in the containment atmosphere which can mostly affect the capture of iodine species. We have highlighted that Ag-MORs with a low Si/Al ratio should be used to ensure the trapping of iodine in presence of VOCs. Remarkably, at low Si/Al ratio, the complete adsorption of I_2 and CH_3I could be achieved in the presence of alcohols, whereas only the adsorption of CH_3I is affected by the presence of aromatic hydrocarbons.

Associated content

Supporting Information. Contains configurations of alcohols adsorbed in Ag-MOR (Si/Al=5=) and computed Bader charges for several systems.

Acknowledgments

This work was performed in the frame of the French research program ANR-11-RSNR-0013-01 called MiRE (Mitigation of Iodine Releases in the Environment). We thank The PMMS (Pôle Messin de Modélisation et de Simulation) and GENCI-CCRT/CINES (Grant No. x2018- A0030810169) for providing us computer time.

Table 1

Computed total interaction energies ΔE_{int}[kJ/mol] of methane (CH4), cyclohexane (C6H12), benzene (C6H6), 1,3-dimethylbenzene (C8H10), methanol (CH3OH), ethanol (C2H5OH), propan-2-ol (C3H7OH) and propanone (C3H6O) with Ag-MORs. The contributions of dispersion energies to the interaction energies ΔEdis[kJ/mol] are reported in this table in parentheses. We note that the site used to adsorb these molecules is found to be in the main channel of mordenite structure.

		ΔE_{int} (ΔE_{dis}) in kJ/mol		
	Si/Al ratio	5	11	47
Iodine species	I_2	-297.6 (-56.0)	-183.8 (-42.9)	-132.6 (-46.5)
	CH_3I	-188.5 (-50.9)	-151.8 (-41.4)	-152.1 (-36.2)
Hydrocarbons	C_8H_{10}	-262.1 (-34.9)	-219.9 (-114.1)	-183.3 (-92.2)
	C_6H_6	-219.4 (-92.1)	-185.1 (-78.9)	-155.8 (-67.7)
	C_6H_{12}	-173.2(-111.3)	-153.9 (-97.3)	-120.3 (-81.8)
	CH_4	-46.6 (-25.1)	-40.5 (-21.8)	-45.7 (-17.0)

Oxygenated molecules	CH_3OH	-117.6 (-32.3)	-111.0 (-29.3)	-106.5 (-24.4)
	C_2H_5OH	-146.4 (-51.4)	-133.7 (-45.8)	-125.3 (-39.5)
	C_3H_7OH	-164.5 (-74.7)	-159.5 (-64.4)	-147.7 (-53.6)
	C_3H_6O	-158.4 (-66.0)	-142.7 (-54.9)	-146.9 (45.9)

Table 2

Distances between Ag cations and aromatic centers of benzene and 1,3-dimethylbenzene in Ag-MOR

Molecules	Si/Al ratio	π-cation bond (Å)
Benzene	5	3.09 ; 3.13 ; 3.27 ; 5.25 ; 5.26 ; 5.42 ; 5.68 ; 5.73
	11	2.89 ; 3.17 ; 5.13 ; 5.36
	47	2.66
1,3-dimethylbenzene	5	2.73 ; 2.79 ; 3.79 ; 4.48 ; 4.91 ; 6.00 ; 6.21 ; 6.40
	11	2.68 ; 3.87 ; 4.227 ; 4.84
	47	2.74

Table 3

DFT and dispersion contributions of oxygen and carbon atoms to the alcohol adsorptions into Ag-MORs.

	Si/Al	CH_3OH	C_2H_5OH	C_3H_7OH
ΔE_{int} (kJ/mol)	5	-117.6	-146.4	-164.5
	11	-111,0	-133.7	-159.5
	47	-106.5	-125.3	-147.7
ΔE_{disp} (kJ/mol)	5	-32.3	-51.4	-74.7
	11	-29.3	-45.8	-64.4
	47	-24.4	-39.5	-53.6
ΔE_{DFT} kJ/mol	5	-85.3	--95.0	-89.8
	11	-81.7	-87.9	-95.1
	47	-82.1	-85.8	-94.1
ΔE_{disp} (CH_x) in kJ/mol	5	-23.4	-46.9	-70.3
	11	-24.3	-48.5	-72.8
	47	-20.6	-41.2	-61.9
ΔE_{disp} (OH) in kJ/mol	5	-8.9	-4.5	-4.4
	11	-5.0	+2.7	+8.4
	47	-3.8	+1.7	+8.3

Table 4

C-O distance (Å) in the gas state and the adsorbed state of methanol, ethanol and propan-2-ol.

	Gaseous state	Adsorbed state in Ag-MOR (Si/Al ratio)		
		Ag-MOR (5)	Ag-MOR (11)	Ag-MOR (47)
CH_3OH	1.43	1.45	1.45	1.45
C_2H_5OH	1.44	1.45	1.46	1.46
C_3H_7OH	1.44	1.49	1.48	1.48

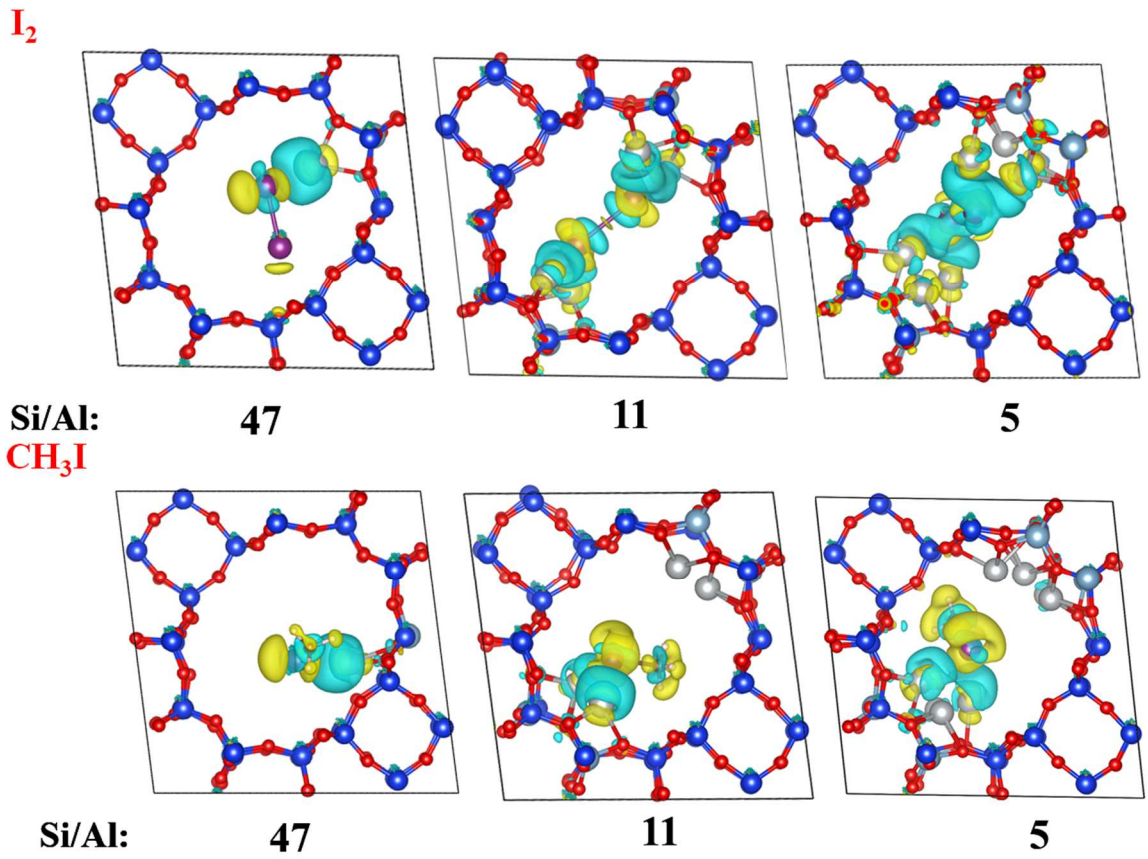

Fig.1. Difference in electronic density (Δρ) induced by adsorption in various Ag-MORs of I_2 (top) and CH_3I (bottom). The blue (yellow) zones indicate density increase (decrease).

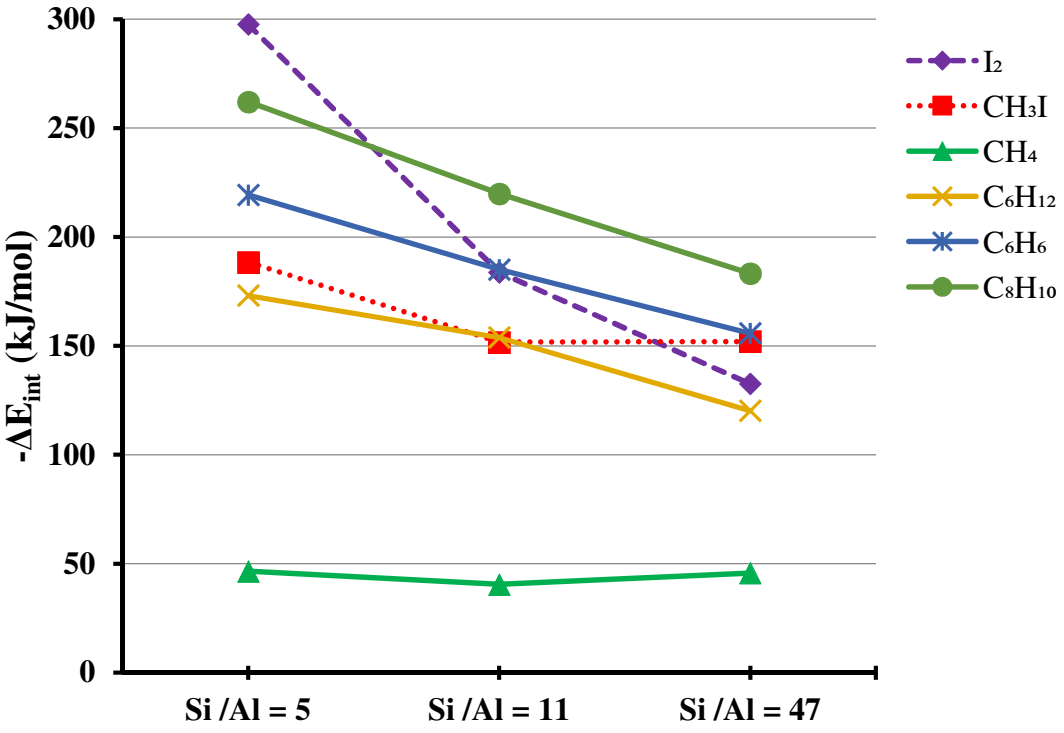

Fig.2. Interaction energies ΔE_{int} (kJ/mol) of the investigated hydrocarbons and iodine species adsorbed on Ag-MOR with three Si/Al ratios of 5, 11 and 47.

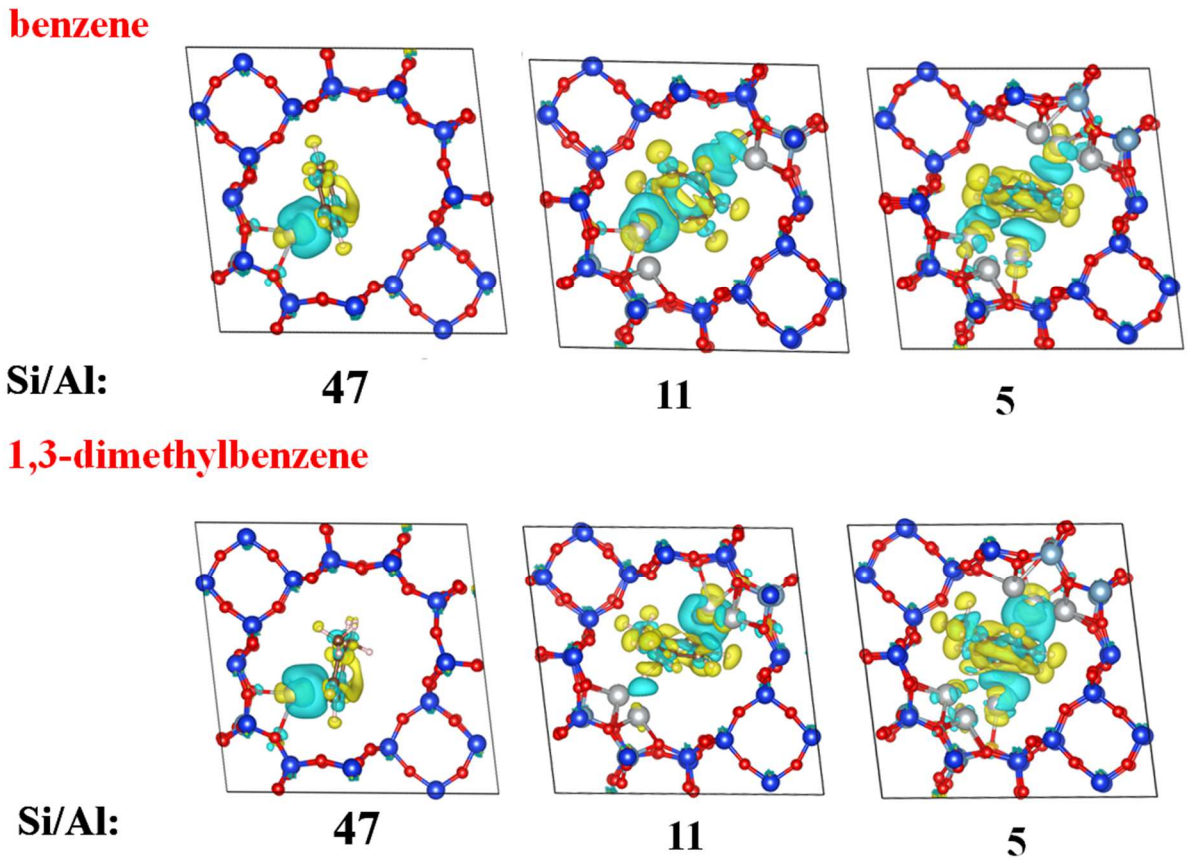

Fig.3. Difference in electronic density (Δρ) induced by adsorption in various Ag-MORs of benzene (top) and 1,3-dimethylbenzene (bottom). The blue (yellow) zones indicate density increase (decrease).

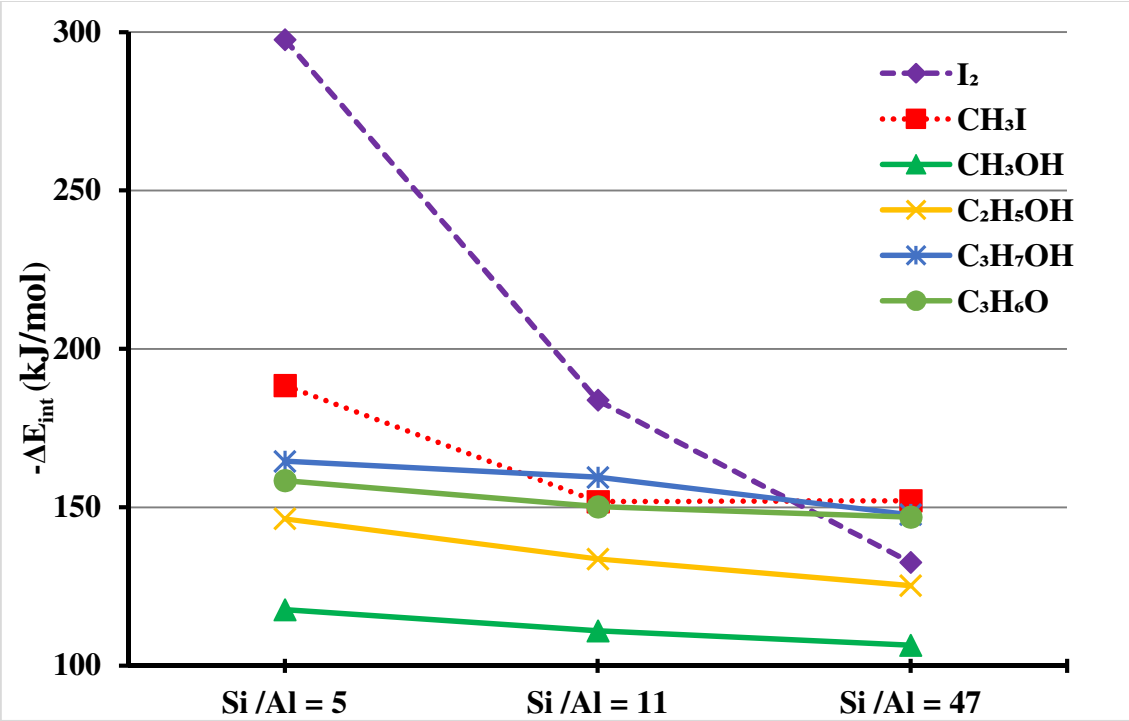

Fig.4. Interaction energies ΔE_{int} (kJ/mol) of the investigated oxygenated and iodine species adsorbed in Ag-MOR with three Si/Al ratios of 5, 11 and 47.

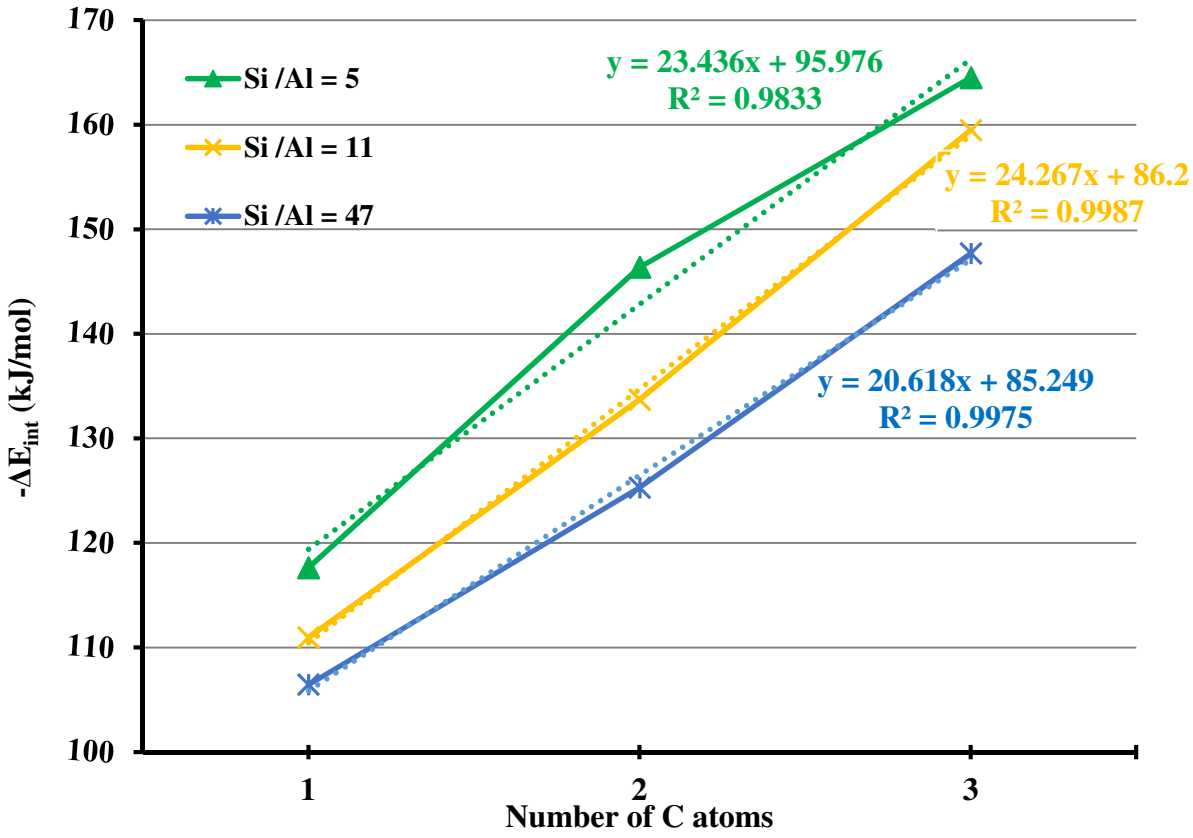

Fig.5. Evolution of the interaction energy of C1 to C3 alcohols with Ag-MOR as a function as their number of carbon atoms for three different Si/Al ratios of 5, 11 and 47.

References

[1] A.J. González, CHERNOBYL VIS-À-VIS THE NUCLEAR FUTURE: AN INTERNATIONAL PERSPECTIVE, Health Phys. 93 (2007) 571. doi:10.1097/01.HP.0000282037.88438.3d.

[2] J. Huve, A. Ryzhikov, H. Nouali, V. Lalia, G. Augé, T.J. Daou, Porous sorbents for the capture of radioactive iodine compounds: a review, RSC Adv. 8 (2018) 29248–29273. doi:10.1039/C8RA04775H.

[3] B.J. Riley, J.D. Vienna, D.M. Strachan, J.S. McCloy, J.L. Jerden, Materials and processes for the effective capture and immobilization of radioiodine: A review, J. Nucl. Mater. 470 (2016) 307–326. doi:10.1016/j.jnucmat.2015.11.038.

[4] Y. Rachuri, K.K. Bisht, E. Suresh, Two-Dimensional Coordination Polymers Comprising Mixed Tripodal Ligands for Selective Colorimetric Detection of Water and Iodine Capture, Cryst. Growth Des. 14 (2014) 3300–3308. doi:10.1021/cg500188n.

[5] S. Ma, S.M. Islam, Y. Shim, Q. Gu, P. Wang, H. Li, G. Sun, X. Yang, M.G. Kanatzidis, Highly Efficient Iodine Capture by Layered Double Hydroxides Intercalated with Polysulfides, Chem. Mater. 26 (2014) 7114–7123. doi:10.1021/cm5036997.

[6] M. Ponce-Vargas, A. Muñoz-Castro, Tiara-like Complexes acting as Iodine Encapsulating Agents: The Role of M···I Interactions in [M(μ-SCH2CO2Me)2]8□I2 (M = Ni, Pd, Pt) Inclusion Compounds, J. Phys. Chem. C. 120 (2016) 23441–23448. doi:10.1021/acs.jpcc.6b08643.

[7] M. Kitamura, K. Funabashi, M. Kikuchi, H. Yusa, Y. Fukushima, S. Horiuchi, Silver-impregnated alumina for removal of radioactive methyl iodide, Trans Am Nucl Soc U. S. 30 (1978). https://www.osti.gov/biblio/6537164 (accessed November 6, 2018).

[8] B. Li, X. Dong, H. Wang, D. Ma, K. Tan, S. Jensen, B.J. Deibert, J. Butler, J. Cure, Z. Shi, T. Thonhauser, Y.J. Chabal, Y. Han, J. Li, Capture of organic iodides from nuclear waste by metal-organic framework-based molecular traps, Nat. Commun. 8 (2017) 485. doi:10.1038/s41467-017-00526-3.

[9] J.G. Jolley, H.G. Tompkins, Desorption of organics from silver zeolite, Appl. Surf. Sci. 21 (1985) 288–296. doi:10.1016/0378-5963(85)90024-8.

[10] D.F. Sava, M.A. Rodriguez, K.W. Chapman, P.J. Chupas, J.A. Greathouse, P.S. Crozier, T.M. Nenoff, Capture of Volatile Iodine, a Gaseous Fission Product, by Zeolitic

Imidazolate Framework-8, J. Am. Chem. Soc. 133 (2011) 12398–12401. doi:10.1021/ja204757x.

[11] S.U. Nandanwar, K. Coldsnow, V. Utgikar, P. Sabharwall, D. Eric Aston, Capture of harmful radioactive contaminants from off-gas stream using porous solid sorbents for clean environment – A review, Chem. Eng. J. 306 (2016) 369–381. doi:10.1016/j.cej.2016.07.073.

[12] W.J. Maeck, D.T. Pence, J.H. Keller, Highly efficient inorganic adsorber for airborne iodine species (silver zeolithe development studies). US Atomic Energy Commission Report IN-1224, 1968 19pp Nucl Sei Abstr. 23 (1969) 2372.

[13] L.N. Rastunov, E.P. Magomedbekov, A.V. Obruchikov, L.A. Lomazova, Evaluation of the sorbent layer thickness in iodine filters, At. Energy. 110 (2011) 68–72. doi:10.1007/s10512-011-9392-6.

[14] K.W. Chapman, P.J. Chupas, T.M. Nenoff, Radioactive Iodine Capture in Silver-Containing Mordenites through Nanoscale Silver Iodide Formation, J. Am. Chem. Soc. 132 (2010) 8897–8899. doi:10.1021/ja103110y.

[15] B. Azambre, M. Chebbi, Evaluation of Silver Zeolites Sorbents Toward Their Ability to Promote Stable CH3I Storage as AgI Precipitates, ACS Appl. Mater. Interfaces. 9 (2017) 25194–25203. doi:10.1021/acsami.7b02366.

[16] S.H. Bruffey, R.T. Jubin, J.A. Jordan, Capture of Elemental and Organic Iodine from Dilute Gas Streams by Silver-exchanged Mordenite, Procedia Chem. 21 (2016) 293–299. doi:10.1016/j.proche.2016.10.041.

[17] E.R. Vance, D.K. Agrawal, X-ray studies of iodine sorption in some silver zeolites, J. Mater. Sci. 17 (1982) 1889–1894. doi:10.1007/BF00540404.

[18] S. Chibani, M. Chebbi, S. Lebègue, T. Bučko, M. Badawi, A DFT investigation of the adsorption of iodine compounds and water in H-, Na-, Ag-, and Cu- mordenite, J. Chem. Phys. 144 (2016) 244705. doi:10.1063/1.4954659.

[19] S. Chibani, M. Chebbi, S. Lebègue, L. Cantrel, M. Badawi, Impact of the Si/Al ratio on the selective capture of iodine compounds in silver-mordenite: a periodic DFT study, Phys. Chem. Chem. Phys. 18 (2016) 25574–25581. doi:10.1039/C6CP05015H.

[20] M. Chebbi, S. Chibani, J.-F. Paul, L. Cantrel, M. Badawi, Evaluation of volatile iodine trapping in presence of contaminants: A periodic DFT study on cation exchanged-faujasite, Microporous Mesoporous Mater. 239 (2017) 111–122. doi:10.1016/j.micromeso.2016.09.047.

[21] T.M. Nenoff, M.A. Rodriguez, N.R. Soelberg, K.W. Chapman, Silver-mordenite for radiologic gas capture from complex streams: Dual catalytic CH3I decomposition and I confinement, Microporous Mesoporous Mater. 200 (2014) 297–303. doi:10.1016/j.micromeso.2014.04.041.

[22] N. Soelberg, T. Watson, Deep Bed Iodine Sorbent Testing FY 2011 Report, Idaho National Laboratory (INL), 2011. doi:10.2172/1042398.

[23] J.C. Wren, D.J. Jobe, G.G. Sanipelli, J.M. Ball, Dissolution of organic solvents from painted surfaces into water, Can. J. Chem. 78 (2000) 464–473. doi:10.1139/v00-042.

[24] J. Liu, X. Zhang, M. Dong, J. Wang, A THEORETICAL STUDY ON ADSORPTION OF THIOPHENE, BENZENE, AND HEXANE IN Na-, Ag-, AND Cu-EXCHANGED MORDENITE, J. Theor. Comput. Chem. 10 (2011) 133–145. doi:10.1142/S0219633611006359.

[25] S. Chibani, I. Medlej, S. Lebègue, J.G. Ángyán, L. Cantrel, M. Badawi, Performance of CuII-, PbII-, and HgII-Exchanged Mordenite in the Adsorption of I2, ICH3, H2O, CO, ClCH3, and Cl2: A Density Functional Study, ChemPhysChem. 18 (2017) 1642–1652. doi:10.1002/cphc.201700104.

[26] A. Alberti, P. Davoli, G. Vezzalini, The crystal structure refinement of a natural mordenite, Z. Für Krist. - Cryst. Mater. 175 (2015) 249–256. doi:10.1524/zkri.1986.175.14.249.

[27] T. Bučko, J. Hafner, The role of spatial constraints and entropy in the adsorption and transformation of hydrocarbons catalyzed by zeolites, J. Catal. 329 (2015) 32–48. doi:10.1016/j.jcat.2015.04.015.

[28] W.J. Mortier, Compilation of Extra Framework Sites in Zeolites (Structure Commission of the International Zeolite Association), Butterworths, London, 1982.

[29] T. Bučko, J. Hafner, L. Benco, Adsorption and vibrational spectroscopy of ammonia at mordenite: Ab initio study, J. Chem. Phys. 120 (2004) 10263–10277. doi:10.1063/1.1737302.

[30] T. Bučko, J. Hafner, L. Benco, Adsorption and Vibrational Spectroscopy of CO on Mordenite: Ab initio Density-Functional Study, J. Phys. Chem. B. 109 (2005) 7345–7357. doi:10.1021/jp050151u.

[31] L. Benco, D. Tunega, Adsorption of H2O, NH3 and C6H6 on alkali metal cations in internal surface of mordenite and in external surface of smectite: a DFT study, Phys. Chem. Miner. 36 (2009) 281–290. doi:10.1007/s00269-008-0276-9.

[32] G. Kresse, J. Hafner, Ab initio molecular dynamics for liquid metals, Phys. Rev. B. 47 (1993) 558–561. doi:10.1103/PhysRevB.47.558.

[33] J.P. Perdew, K. Burke, M. Ernzerhof, Generalized Gradient Approximation Made Simple, Phys. Rev. Lett. 77 (1996) 3865–3868. doi:10.1103/PhysRevLett.77.3865.

[34] P.E. Blöchl, Projector augmented-wave method, Phys. Rev. B. 50 (1994) 17953–17979. doi:10.1103/PhysRevB.50.17953.

[35] G. Kresse, D. Joubert, From ultrasoft pseudopotentials to the projector augmented-wave method, Phys. Rev. B. 59 (1999) 1758–1775. doi:10.1103/PhysRevB.59.1758.

[36] A. Tkatchenko, M. Scheffler, Accurate Molecular Van Der Waals Interactions from Ground-State Electron Density and Free-Atom Reference Data, Phys. Rev. Lett. 102 (2009) 073005. doi:10.1103/PhysRevLett.102.073005.

[37] T. Bučko, S. Lebègue, J. Hafner, J.G. Ángyán, Improved Density Dependent Correction for the Description of London Dispersion Forces, J. Chem. Theory Comput. 9 (2013) 4293–4299. doi:10.1021/ct400694h.

[38] T. Bučko, S. Lebègue, J.G. Ángyán, J. Hafner, Extending the applicability of the Tkatchenko-Scheffler dispersion correction via iterative Hirshfeld partitioning, J. Chem. Phys. 141 (2014) 034114. doi:10.1063/1.4890003.

[39] K. Momma, F. Izumi, VESTA: a three-dimensional visualization system for electronic and structural analysis, J. Appl. Crystallogr. 41 (2008) 653–658. doi:10.1107/S0021889808012016.

[40] R.F. Bader, Atoms in molecules: a quantum theory, vol 22, International series of monographs on chemistry, Oxford University Press, Oxford, 1990.

[41] W. Tang, E. Sanville, G. Henkelman, A grid-based Bader analysis algorithm without lattice bias, J. Phys. Condens. Matter. 21 (2009) 084204. doi:10.1088/0953-8984/21/8/084204.

[42] E. Sanville, S.D. Kenny, R. Smith, G. Henkelman, Improved grid-based algorithm for Bader charge allocation, J. Comput. Chem. 28 (2007) 899–908. doi:10.1002/jcc.20575.

[43] G. Henkelman, A. Arnaldsson, H. Jónsson, A fast and robust algorithm for Bader decomposition of charge density, Comput. Mater. Sci. 36 (2006) 354–360. doi:10.1016/j.commatsci.2005.04.010.

[44] T. Bučko, S. Chibani, J.-F. Paul, L. Cantrel, M. Badawi, Dissociative iodomethane adsorption on Ag-MOR and the formation of AgI clusters: an ab initio molecular dynamics study, Phys. Chem. Chem. Phys. 19 (2017) 27530–27543. doi:10.1039/C7CP05562E.

[45] G. Witte, S. Lukas, P.S. Bagus, C. Wöll, Vacuum level alignment at organic/metal junctions: “Cushion” effect and the interface dipole, Appl. Phys. Lett. 87 (2005) 263502. doi:10.1063/1.2151253.

[46] A. Bilić, J.R. Reimers, N.S. Hush, R.C. Hoft, M.J. Ford, Adsorption of Benzene on Copper, Silver, and Gold Surfaces, J. Chem. Theory Comput. 2 (2006) 1093–1105. doi:10.1021/ct050237r.

[47] T.S. Chwee, M.B. Sullivan, Adsorption studies of C_6H_6 on Cu (111), Ag (111), and Au (111) within dispersion corrected density functional theory, J. Chem. Phys. 137 (2012) 134703. doi:10.1063/1.4755993.

[48] M.C. Tsai, E.L. Muetterties, Platinum metal surface chemistry of benzene and toluene, J. Am. Chem. Soc. 104 (1982) 2534–2539. doi:10.1021/ja00373a034.

[49] V.H. Grassian, E.L. Muetterties, Vibrational electron energy loss spectroscopic study of benzene, toluene, and pyridine adsorbed on palladium(111) at 180 K, J. Phys. Chem. 91 (1987) 389–396. doi:10.1021/j100286a028.

[50] R.S. Mulliken, W.B. Person, Molecular complexes: a lecture and reprint volume, Wiley-Interscience, 1969.

[51] P. Kozyra, J. Załucka, M. Mitoraj, E. Brocławik, J. Datka, From Electron Density Flow Towards Activation: Benzene Interacting with Cu(I) and Ag(I) Sites in ZSM-5. DFT Modeling, Catal. Lett. 126 (2008) 241–246. doi:10.1007/s10562-008-9620-4.

[52] M. Munakata, L.P. Wu, T. Kuroda-Sowa, M. Maekawa, Y. Suenaga, G.L. Ning, T. Kojima, Supramolecular Silver(I) Complexes with Highly Strained Polycyclic Aromatic Compounds, J. Am. Chem. Soc. 120 (1998) 8610–8618. doi:10.1021/ja981483y.

[53] M. Munakata, L.P. Wu, T. Kuroda-Sowa, M. Maekawa, Y. Suenaga, K. Sugimoto, Construction and Conductivity of W-Type Sandwich Silver(I) Polymers with Pyrene and Perylene, Inorg. Chem. 36 (1997) 4903–4905. doi:10.1021/ic9706360.

[54] E.A.H. Griffith, E.L. Amma, Metal ion-aromatic complexes. XX. Preparation and molecular structure of anthracenetetrakis(silver perchlorate) monohydrate, J. Am. Chem. Soc. 96 (1974) 5407–5413. doi:10.1021/ja00824a015.

[55] Y. Suda, Interaction of benzene, cyclohexene, and cyclohexane with the surface of titanium dioxide (rutile), Langmuir. 4 (1988) 147–152. doi:10.1021/la00079a027.

[56] D. Barthomeuf, B.-H. Ha, Adsorption of benzene and cyclohexane on faujasite-type zeolites. Part 2.—Adsorption site efficiency and zeolite field influence at high coverage, J. Chem. Soc. Faraday Trans. 1 Phys. Chem. Condens. Phases. 69 (1973) 2158–2165. doi:10.1039/F19736902158.

[57] B.G. Aristov, V. Bosacek, A.V. Kiselev, Dependence of adsorption of krypton and xenon by crystals of zeolite LiX and NaX on pressure and temperature, Trans. Faraday Soc. 63 (1967) 2057–2067. doi:10.1039/TF9676302057.